

# Active Earth Pressure on Inclined Retaining Walls in Static and Pseudo-Static Conditions

A. Ghanbari<sup>1,\*</sup> and M. Ahmadabadi<sup>1</sup>

Received: May 2009

Accepted: April 2010

**Abstract:** Inclined retaining walls with slopes less than perpendicular are appropriate candidates in several engineering problems. Yet, to the knowledge of authors, only a few analytical solution for calculation of active earth pressure on such walls, which will be usually smaller than the same pressure on vertical ones, has been presented neither in research papers nor in design codes. Considering limit equilibrium concept in current research, a new formulation is proposed for determination of active earth pressure, angle of failure wedge and application point of resultant force for inclined walls. Necessary parameters are extracted assuming the pseudo-static seismic coefficient to be valid in earthquake conditions. Moreover, based on Horizontal Slices Method (HSM) a new formulation is obtained for determining the characteristics of inclined walls in granular and or frictional cohesive soils. Findings of present analysis are then compared with results from other available methods in similar conditions and this way, the validity of proposed methods has been proved. Finally according to the results of this research, a simplified relation for considering the effect of slope in reduction of active earth pressure and change in failure wedge in inclined retaining walls has been proposed.

**Keywords:** Active earth pressure, inclined retaining wall, Horizontal Slices Method, Limit equilibrium, Pseudo-static seismic coefficient

## 1. Introduction

Inclined retaining walls are employed in many engineering projects such as spillway of dams or costal structures. The value of active earth pressure has direct relation to the angle of wall. It means by reduction of inclination angle from vertical state the value of active earth pressure will decrease. Pressure distribution along wall, critical angle of failure wedge and the application point of resultant force are all dependants on the slope of wall. However only a few analytical solutions has been reported in design coeds or published researches for calculating the active earth pressure which is usually smaller in inclined walls than vertical walls. Using analytical relations based on equilibrium of forces and moments in a failure wedge, characteristics of active earth pressure in static and pseudo-static conditions for inclined walls is investigated in this research.

Recent studies of geotechnical structures include experimental studies, numerical analysis and analytical models [1-4]. For many decades, the seismic analysis of retaining walls has been

performed by a simple extension of coulomb's limit-equilibrium technique widely known as the Mononobe and Matsuo [5] and Okabe [6] procedure (M-O method). This technique is an extension of coulomb's method in static conditions for calculating the earth pressure by considering equilibrium of triangular failure wedge. Based on M-O method, Zarrabi-Kashani [7] proposed a formulation for determining the angle of critical wedge in seismic conditions.

Several researchers have studied the problem of earthquake induced lateral earth pressure from various points of view for example Mononobe and Matsuo [5] by considering the Coulomb's mechanism, Morison and Ebeling [8] by applying the limit equilibrium concept with logarithmic spiral failure surface, Soubra [9] by using upper bound limit analysis, Chen [10] with LRFD method, Kumar [11] and Kumar and Chitikela [12], Cheng [13] by employing the slip line method and Yang and Yin [14] by applying limit analysis method and with nonlinear failure criterion. Considering the effects of both horizontal and vertical seismic coefficients, Choudhury and Nimbalkar [15] investigated the temporal effect and phase change in shear and primary waves propagating through the backfill behind a rigid wall. Mylonakis et al. [16] suggested another solution based on theory of plasticity for calculation of gravitational and

---

\* Corresponding author: Email: Ghanbari@tmu.ac.ir

<sup>1</sup> Faculty of Engineering, Tarbiat Moallem University, No. 49 Mofatteh Ave., Tehran, I.R. Iran

earthquake-induced earth pressure on gravity walls with retaining cohesionless soil. Yepes et al. [17] have examined the economic optimization of reinforced concrete earth-retaining walls used in road construction. The simulated annealing algorithm was the proposed method to optimize walls.

In this paper, two new formulas for inclined retaining walls are presented. The former is based on limit equilibrium concept for cohesionless backfills. Modifying equations and unknowns of Horizontal Slices Method [18-23] the later formula is a new approach for calculation of static and seismic active earth pressure behind inclined retaining walls with cohesive-frictional backfill. Overcoming some limitations in previous methods, in both of mentioned procedures an attempt has been done to investigate the problem of inclined retaining walls which has not been specifically dealt up to now.

## 2. Limit equilibrium method for cohesionless soils

In order to find analytical relations for calculating the active earth pressure acting on an inclined wall, applied forces on failure wedge are assumed as illustrated in Fig. 1. When being considered for a granular soil, there will be three unknowns in depicted system which can be determined by solving two equilibrium equations of forces, in horizontal and vertical directions, in addition of an extra relation. The further equation is constructed based on the fact that maximum active earth pressure is caused within the failure wedge and thus makes the value of  $\frac{\partial \beta}{\partial P_{ae}}$  being equal to zero. The equations and unknowns are noted in Table 1. In the Fig. 1,  $\beta$  is defined as the

**Table 1.** Equations and unknowns for an inclined retaining wall with unreinforced frictional backfill

Unknowns	Number	Equations	Number
$P_{ae}$	1	$\sum F_x = 0$	1
$F$	1	$\sum F_y = 0$	1
$\beta$	1	$\frac{\partial \beta}{\partial P_{ae}} = 0$	1

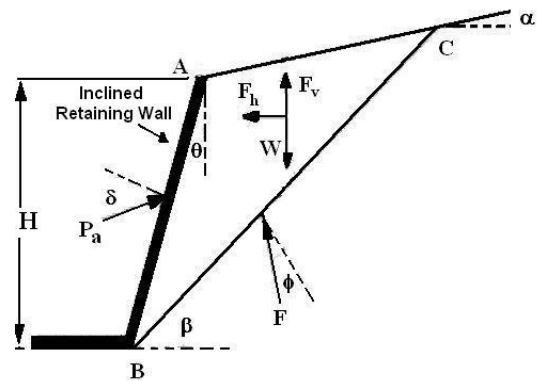


**Fig. 1.** Equilibrium of forces in hypothetical failure wedge angle of failure wedge with horizon.

Equilibrium equations are resulted as follows:

$$\sum F_x = 0 \Rightarrow P_{ae} \cos \delta \cos \theta + P_{ae} \sin \delta \sin \theta - F_h + F \sin \varphi \cos \beta - F \cos \varphi \sin \beta = 0 \quad (1)$$

$$\sum F_y = 0 \Rightarrow P_{ae} \sin \delta \cos \theta - P_{ae} \cos \delta \sin \theta + F_v - W + F \sin \varphi \sin \beta + F \cos \varphi \cos \beta = 0 \quad (2)$$

Horizontal and vertical forces as well as the weight of failure wedge can be calculated with equations (3), (4) and (5):

$$F_h = K_h W, \quad K_v = \frac{\alpha_v}{g} \quad (3)$$

$$F_v = K_v W, \quad K_h = \frac{\alpha_h}{g} \quad (4)$$

$$W = \frac{1}{2} \gamma H^2 \frac{\cos(\theta + \alpha) \cos(\theta + \beta)}{\cos^2(\theta) \sin(\beta - \alpha)} \quad (5)$$

Substituting equation (5) into equations (1) and (2), applied force on the wall will be determined as follows:

$$F(\beta) = \frac{K_h W \cos(\beta - \varphi)}{\cos(\theta - \delta - \varphi + \beta)} - \frac{K_v W \sin(\beta - \varphi)}{\cos(\theta - \delta - \varphi + \beta)} + \frac{W \sin(\beta - \varphi)}{\cos(\theta - \delta - \varphi + \beta)} \quad (6)$$

Equation (6) is consisted of three terms. First

one, in the left, shows the effect of seismic horizontal force. Midterm is related to the earthquake's vertical force and the last term, in the right, considers the static force due to weight of failure wedge. Substitution of wedge's weight in equation 6 leads to following relations for calculating the applied force on an inclined wall:

$$P_{ae}(\beta) = \frac{1}{2} \gamma H^2 \frac{\cos(\theta + \alpha) \cos(\theta + \beta) \sin(\beta - \varphi)}{\cos^2(\theta) \sin(\beta - \alpha) \cos(\theta - \delta - \varphi + \beta)} \quad (7)$$

$$\cdot \left[ \frac{K_h}{\tan(\beta - \varphi)} + (1 - K_v) \right]$$

$$K_{ae}(\beta) = \frac{\cos(\theta + \alpha) \cos(\theta + \beta) \sin(\beta - \varphi)}{\cos^2(\theta) \sin(\beta - \alpha) \cos(\theta - \delta - \varphi + \beta)} \quad (8)$$

$$\left[ \frac{K_h}{\tan(\beta - \varphi)} + (1 - K_v) \right]$$

$$P_{ae} = \frac{1}{2} \gamma H^2 K_{ae} \quad (9)$$

Solving equation (10) with trial and error will result in critical angle of wedge.

$$ADB\sqrt{1-C^2} + D\sqrt{1-A^2B^2C^2} - DCB\sqrt{1-A^2} - \quad (10)$$

$$\cdot EB\sqrt{1-A^2C^2} = 0$$

where coefficients of A, B, C, D and E are

defined as follows:

$$A = \sin(\theta + \beta)$$

$$B = \sin(\beta - \alpha)$$

$$C = \sin(\theta - \delta - \varphi + \beta)$$

$$D = K_h \cos(\beta - \varphi) + (1 - K_v) \sin(\beta - \varphi)$$

$$E = K_h \sin(\varphi - \beta) + (1 - K_v) \cos(\beta - \varphi)$$

Neglecting the vertical component of earthquake's force, critical angle of wedge can be calculated with equation (11):

$$\beta = \phi + \text{Arc tan} \frac{-C(K_v) + AB \pm \sqrt{(1 + CK_v)(A - K_v)(1 + AB)(B - C)}}{C + ABC - B - BC(K_v)} \quad (11)$$

where coefficients of A, B and C are defined as follows:

$$A = \tan(\phi - \alpha)$$

$$B = \tan(\phi + \theta)$$

$$C = \tan(\theta - \delta)$$

Using equation (11), angle of failure wedge against  $\beta$  (inclination slope of the wall) is plotted in Fig. 2 for different friction angles. In this figure, linear relation between  $\beta$  and  $\theta$  is

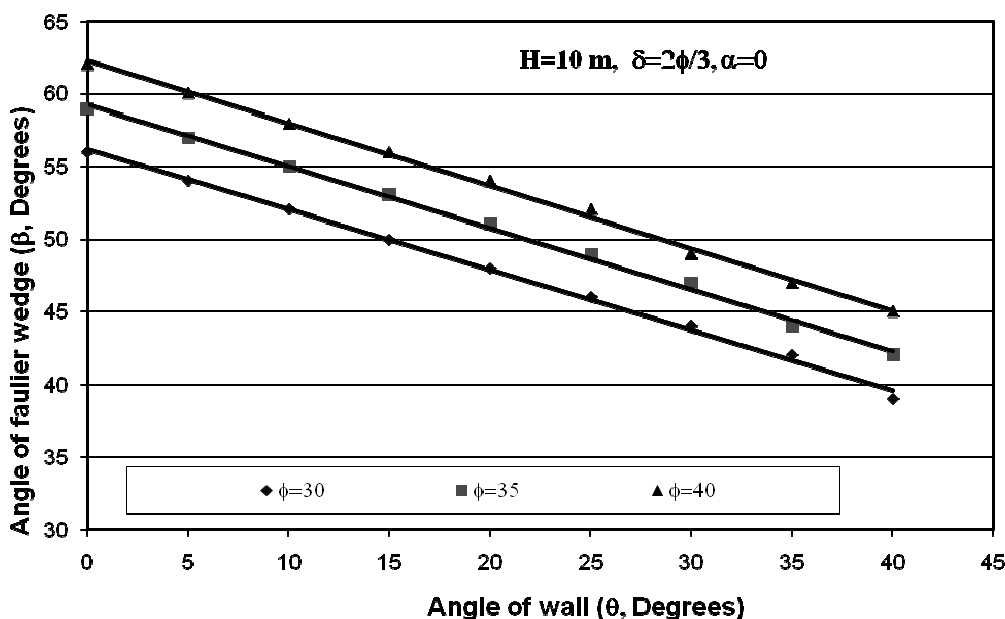


Fig. 2. Angle of failure wedge versus angle of inclination for different internal friction angles

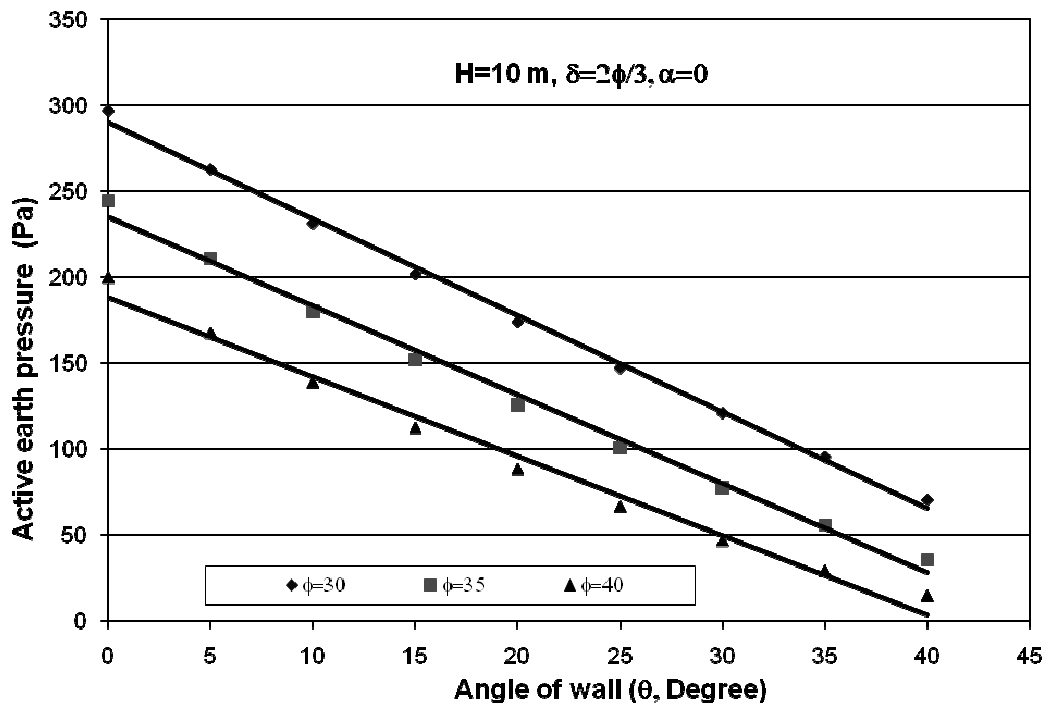


Fig. 3. Active earth pressure against angle of inclination for different internal friction angles

distinguished with satisfactory precision in ordinary conditions.

$$c_1 = 0.0017\phi + 0.36 \quad c_2 = 0.61\phi + 37.7 \quad (13)$$

$$\beta = c_1\theta + c_2 \quad (12)$$

where  $\beta$  and  $\theta$  are in degrees and  $C_1$  and  $C_2$  are calculated by following simplified equation:

Using equation 11, active earth pressure versus angle of inclination for different internal friction angles is plotted in Fig. 3. As can be observed in this figure, an increase in the slope of wall causes

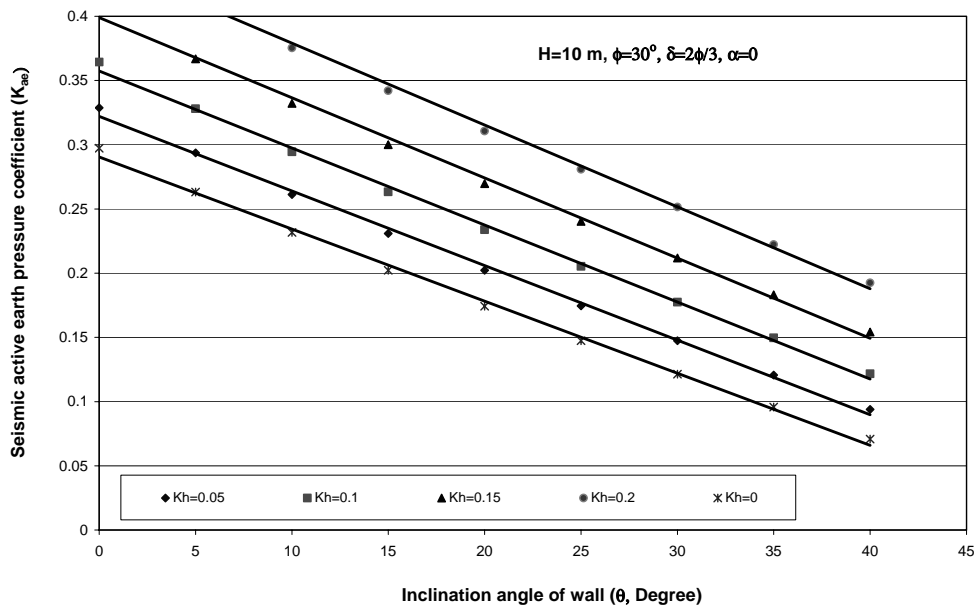


Fig. 4. Seismic active earth pressure versus angle of inclination for different pseudo-static acceleration coefficients

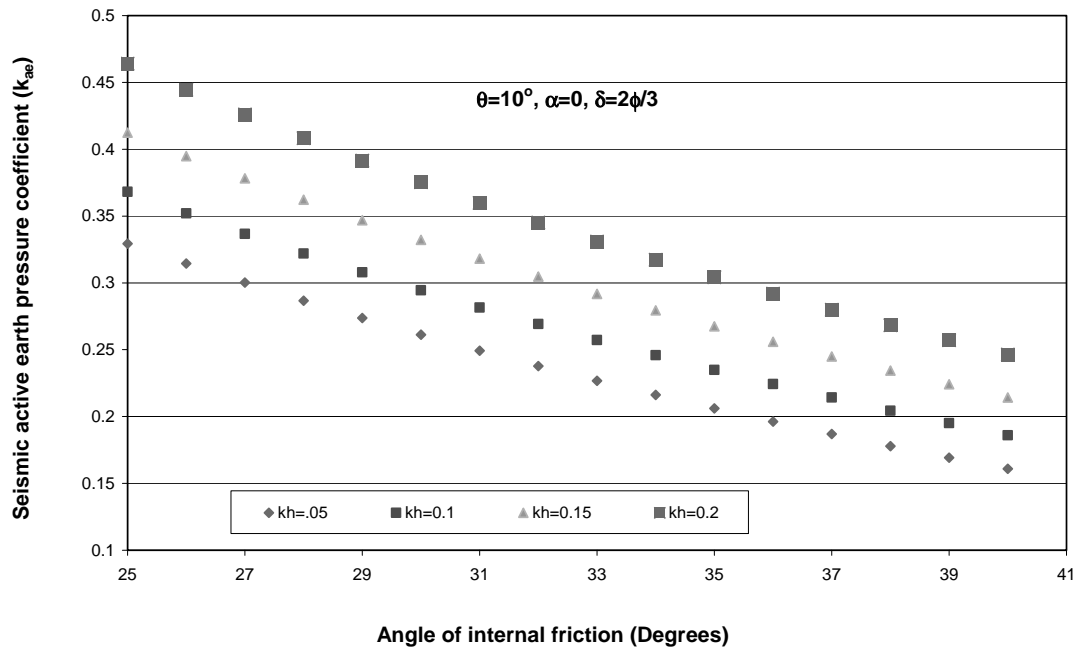


Fig. 5.  $K_{ae}$  against internal friction angle for different pseudo-static coefficients

the reduction of active earth pressure coefficient in static conditions. Fig. 4 also shows seismic active earth pressure versus slope of the wall for different internal friction angles. Since these charts demonstrate the linear variation of mentioned parameters, following relations are suggested for calculating  $K_a$  and  $K_{ae}$  as functions of inclination angle of wall ( $\theta$ ).

$$K_{ae} = (K_{ae})_v \{1 - \theta / \lambda\} \quad (14)$$

$$K_{ae} = (K_{ae})_v \{1 - \theta / \lambda_e\} \quad (15)$$

where  $(K_a)_v$  and  $(K_{ae})_v$  are active earth pressures for a vertical wall in static and seismic conditions, respectively. Also,  $\lambda$  and  $\lambda_e$  are angles of backfill soil at natural stability in static and seismic conditions.

Variation of  $K_{ae}$  versus internal friction angle for a wall with 10 degrees of inclination is plotted in Fig. 5 which shows that by increase in the slope of wall active earth pressure reduces with approximate linear trend. Fig. 6 shows the increase in  $K_{ae}$  with increase in horizontal pseudo-static acceleration coefficient. As can be observed in this figure, the general trend of variations can be assumed as linear with high degree of accuracy in practical applications.

Ratio of pseudo-static acceleration coefficient belonging to vertical and horizontal direction for a wall with 20 degree of inclination is plotted in Fig. 7. This figure shows that with increase in mentioned ratio the value of  $K_{ae}$  increases so that in a constant ratio for all accelerations ratio.

The influence of vertical and horizontal acceleration coefficients on active earth pressure of an inclined wall is shown in Fig. 8, in all of which linear increase of pressure by increase in depth of wall can be observed. This linear response is caused by limit equilibrium assumptions. Non-linear trend in the same condition will be shown further when Horizontal Slices Method is employed as a new approach for calculation of active earth pressure.

### 3. Horizontal Slices Method (HSM) for Cohesive Frictional Backfills

The slices method was originally employed for estimation of slope stability. The most conventional technique for such estimation is vertical slices method. Another solution has also been introduced by Shahgholi et al. [18]. Complete formulation of HSM has been developed by Nouri et al. [19,21]. Seismic acceleration coefficient at different elevations in a structure can be addressed by this method. Azad

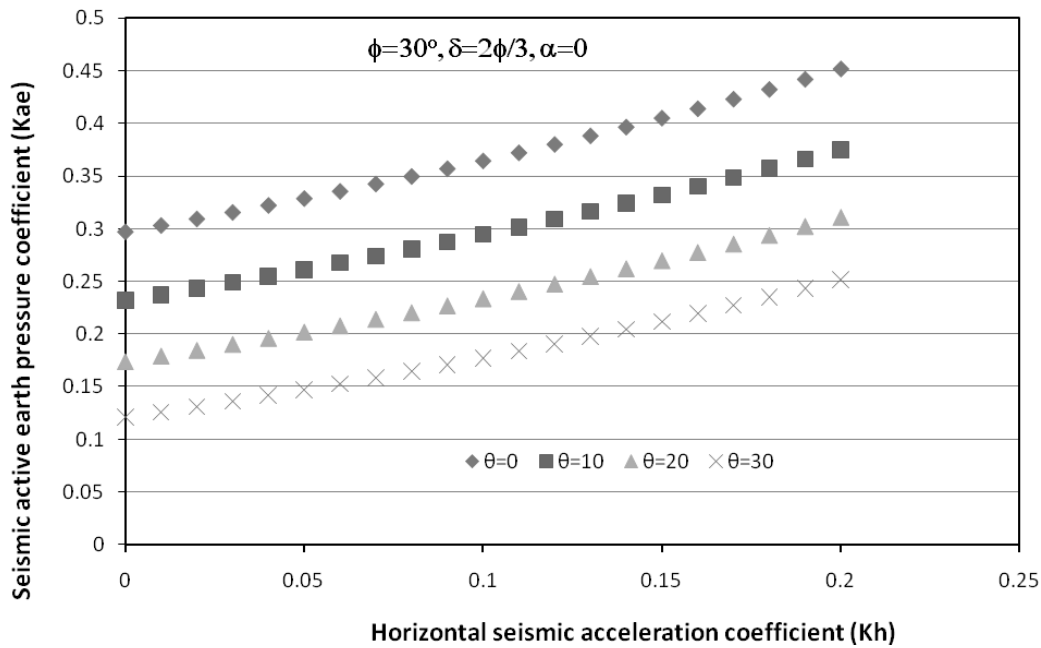


Fig. 6. Variation of Kae versus different horizontal acceleration coefficients (Kh)

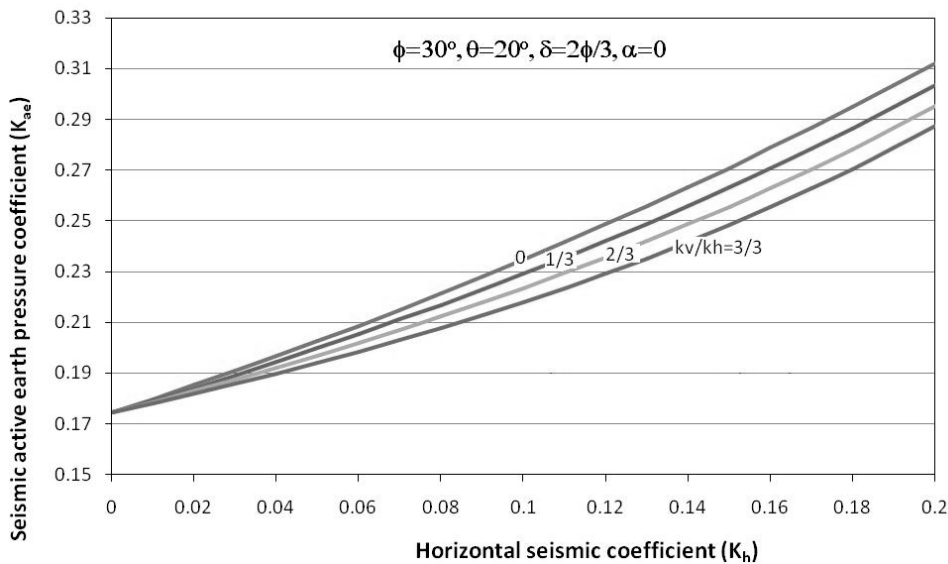


Fig. 7. Variation of Kae versus horizontal seismic coefficient (Kh) for different Kv/Kh ratio

et al. [22], Shekarian et al. [20], and Shekarian and Ghanbari [23] contributed the concept of HSM within the framework of pseudo-dynamic and pseudo-static methods to calculate seismic active earth pressure on retaining walls. Distribution of seismic active earth pressure and the application point of resultant force can both be handled by HSM.

This section deals with a new formulation,

based on Horizontal Slices Method, for studying the applied pressure on inclined walls. Comparison of results obtained from this formulation with the method explained in previous section and also with other formulas reported in literature has been carried out. For this purpose, an inclined retaining wall is considered as illustrated in Fig. 9. The backfill soil has been divided into n horizontal slices for

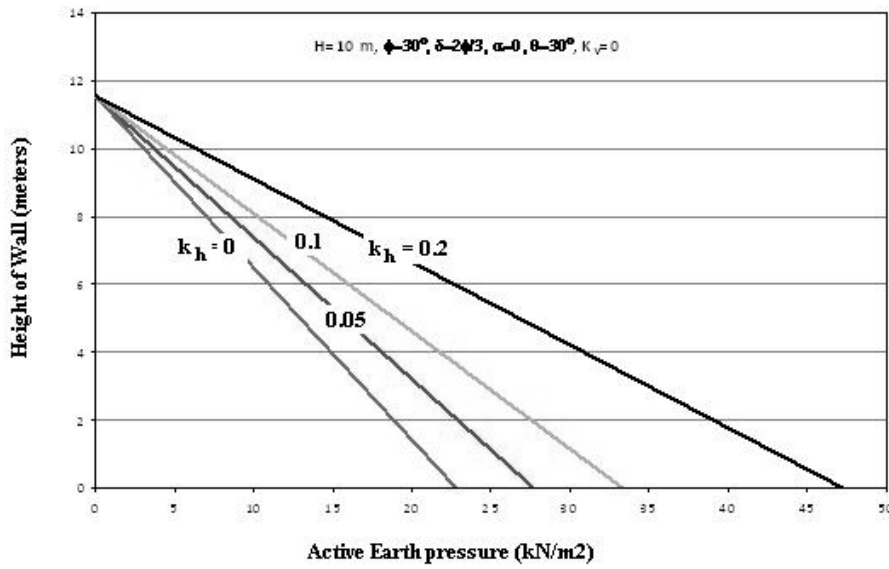


Fig. 8. Pressure distribution along an inclined wall for different horizontal acceleration coefficients

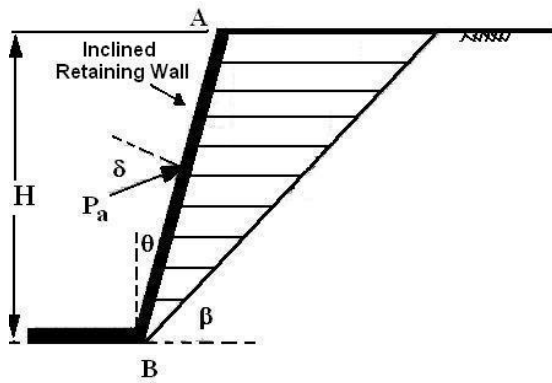


Fig. 9. Division of failure wedge into horizontal slices for an inclined retaining wall

$$h_i = \frac{H}{n} \quad (16)$$

Considering geometrical principles, the distances shown in Fig. 10 will be determined as follows:

$$X_{1i} = \frac{\sum_{j=1}^i h_j}{\tan(\beta)} \quad (17)$$

$$X_{2i} = \left[ \sum_{j=i}^n h_j \right] \tan(\theta) \quad (18)$$

$$X_{1_{i+1}} = \frac{\sum_{j=i+1}^n h_j}{\tan(\beta)} \quad (19)$$

$$X_{3i} = \frac{h(i)}{\tan \beta} \quad (20)$$

all of which the free diagram is plotted as can be observed in Fig. 10.

Having  $n$  slices, it can be written:

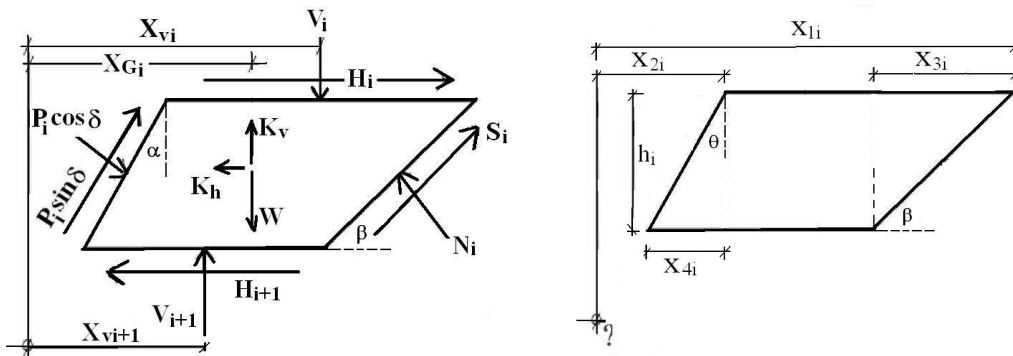


Fig. 10. Diagram of forces in  $i$ th slice and their distance from the point of rotation

**Table 2.** Outline of equations and unknowns for an inclined retaining wall with cohesive–frictional backfill

<i>Unknowns</i>	<i>Number</i>	<i>Equations</i>	<i>Number</i>
$H_i$ <i>Inter-slice shear force</i>	$n$	$\sum F_x = 0$ <i>For each slice</i>	$n$
$N_i$ <i>Normal forces at base of each slice</i>	$n$	$\sum F_y = 0$ <i>For each slice</i>	$n$
$S_i$ <i>Shear forces at base of each slice</i>	$n$	$\sum M_o = 0$ <i>For each slice</i>	$n$
$P_i$ <i>Net force on wall</i>	$n$	$S_i = N_i(\tan\phi + c_i)$ <i>For each slice</i>	$n$

$$X_{4i} = h(i) \tan \theta \quad (21)$$

$$X_{G_i} = \frac{x_{1i}}{2} + \frac{x_{2i}}{2} - \frac{x_{3i}}{4} - \frac{x_{4i}}{4} \quad (22)$$

Weight of each slice can be calculated with equation (23):

$$W_i = \{(X_{1i} - X_{2i} - X_{3i}) + 0.5(X_{3i} + X_{4i})\}h_i\gamma_i \quad (23)$$

In order to determine  $V_i$  and  $V_{i+1}$ , the relation proposed by Segrestin [24] has been applied:

$$V_i = \gamma z_i \cdot \tanh(au + b) \quad (24)$$

Above equation yields more accurate results for inclined masses than the general relation of  $\sigma_v = \gamma h$ . In the Fig. 11,  $X$  and  $Z$  are the horizontal distance from the coordinate center and depth of the point considered, respectively. Parameters  $a$ ,  $b$  and  $u$  can be determined with following equations:

$$a = 2 \tan\left(\frac{\pi}{2} - \theta\right) \cdot \log\left(\frac{2K_a}{K_a + K_b}\right) \quad (25)$$

$$b = \left(\log \frac{K_a + K_\alpha}{K_a - K_\alpha}\right) / 2 \quad (26)$$

$$u_i = \frac{x_j}{z_i} \quad (27)$$

$$K_b = \left[ \frac{\sin\left(\frac{\pi}{2} - \theta - \phi\right)}{\cos(\theta) + \sqrt{\cos(\theta) \cos\left(\frac{\pi}{2} - \theta - \phi\right) \sin \phi}} \right]^2 \quad (28)$$

$$K_a = \tan^2\left(45 - \frac{\phi}{2}\right) \quad (29)$$

The following assumptions have been made:

- Application point of vertical inter-slice force is the center of pressure in stress distribution pattern of that slice.
- Failure surface is considered to be plane.
- Analysis is done on the basis of limit equilibrium concept.
- Proposed method will be applicable only for homogeneous soils.
- Failure surface is assumed to pass through the heel of wall.
- Horizontal inter-slice force is ignored ( $H_i = H_{i-1}$ ) in all of formulas.
- $N_i$  force acts on the midpoint of each slice's base.
- $P_i$  force acts on the midpoint along the height of each slice.

There are  $4n$  equations and  $4n$  unknowns, shown in Table 2, which solving them determines the active earth pressure on an inclined retaining wall.

Equilibrium equations are as follows:

$$\sum F_x = 0 \longrightarrow H_i - H_{i+1} - F_h + S_i \cos \beta - \quad (30)$$

$$N_i \sin \beta + P_i \cos \delta \cos \theta + P_i \sin \delta \sin \theta = 0$$



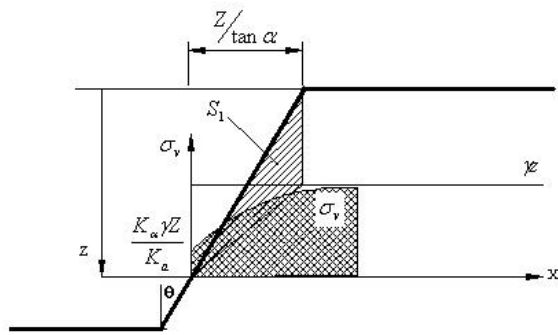


Fig. 11. Vertical stress distribution on horizontal surfaces

$$\sum F_y = 0 \rightarrow -V_i + V_{i+1} + F_v - W_i + S_i \sin \beta \quad (31)$$

$$+ N_i \cos \beta - P_i \cos \delta \sin \theta + P_i \sin \delta \cos \theta = 0$$

$$\sum M_o = 0 \rightarrow V_i X_{V_i} + V_{i+1} X_{V_{i+1}} + (F_h - W_i) X_G + \left[ F_h + \frac{N_i}{\sin \beta} \right] \quad (31)$$

$$- \frac{P_i \cos \delta}{\cos \theta} \times \left[ \sum_{j=i+1}^n h_j + \frac{h_i}{2} \right] + H_{i+1} \sum_{j=i+1}^n h_j - H_i \sum_{j=i}^n h_j = 0$$

$$S_i = [N_i \tan \phi + Cl_i] \quad (33)$$

Where  $c$  is cohesion strength of soil and  $l_i$  can be calculated as follow:

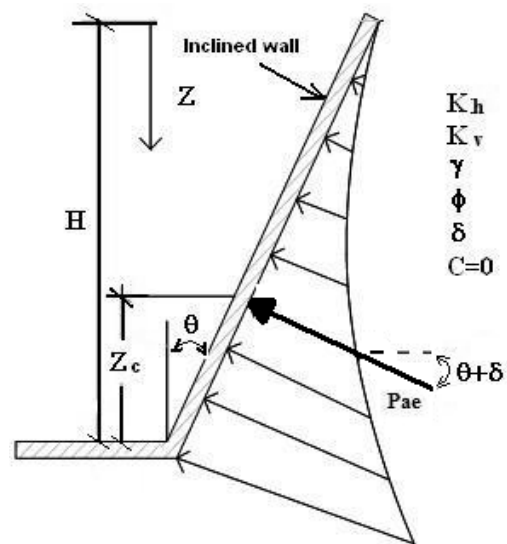


Fig. 12. Stress distribution driven by earthquake

$$l_i = h_i / \sin \beta \quad (34)$$

Having  $P_i$  for each slice, resultant force ( $P$ ) will be achieved by following equation:

$$P = \sum_{i=1}^n P_i \quad (35)$$

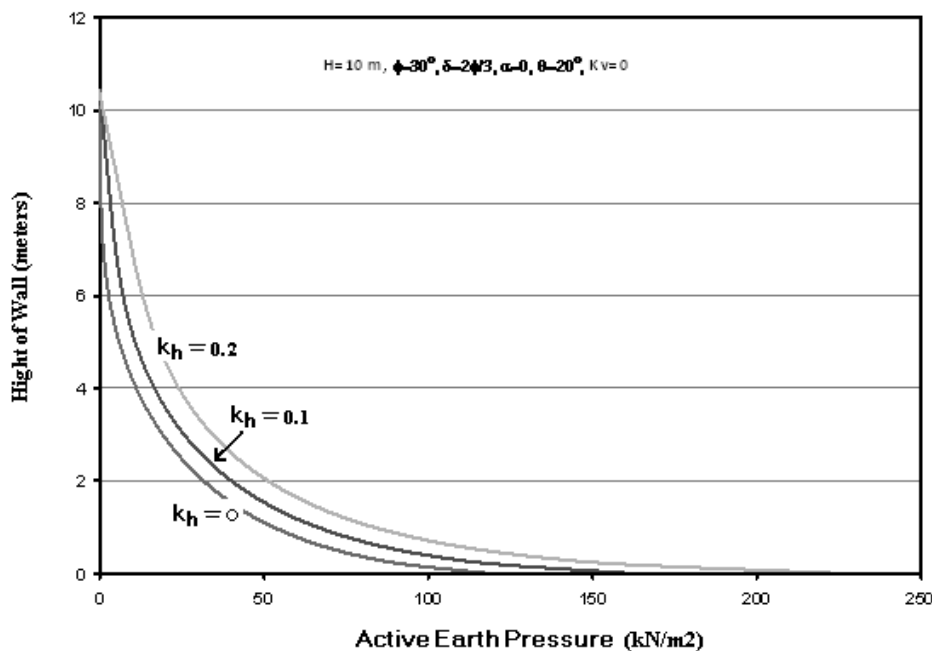


Fig. 13. Stress distribution for different horizontal pseudo-static acceleration coefficients

**Table 3.** Comparison of two proposed methods for calculation of earthquake-induced pressure

LEM: Proposed Method (Based on Limit equilibrium)  
 HSM: Proposed Method (Horizontal slice method)  
 $\gamma = 20 \text{ kN} / \text{m}^3, \alpha = 0^\circ, K_v = 0, c = 0, \delta = 2\phi / 3, \phi = 30^\circ$

$\theta$		$K_h=0$			$K_h=.05$			$K_h=0.1$			$K_h=0.2$		
		$K_a$	$\beta$	$Z_c$	$K_a$	$\beta$	$Z_c$	$K_a$	$\beta$	$Z_c$	$K_a$	$\beta$	$Z_c$
20	LEM	0.174	48	3.33	0.203	46	3.33	0.235	44	3.33	0.312	39	3.33
	HSM	0.180	47.4	1.49	0.216	45.6	1.69	0.256	43.7	1.84	0.356	39.7	2.05
10	LEM	0.232	52	3.33	0.262	50	3.33	0.296	47	3.33	0.377	42	3.33
	HSM	0.230	50.7	2.08	0.268	48.7	2.30	0.306	46.7	2.48	0.400	42	2.76

**Table 4.** Comparison of results for calculation of active earth pressure coefficient

LEM: Proposed Method (Based on Limit equilibrium)  
 HSM: Proposed Method (Horizontal slice method)  
 M-O: Mononobe-Okabe(1929) Zarabi-Kashani(1979),  
 Chang : Chang(2003)  
 $\alpha = 0^\circ, K_v = 0, c = 0, \delta = \frac{2}{3}\phi, \theta = 0$

$\phi$	$K_h=0$				$K_h=0.05$				$K_h=0.1$				$K_h=0.2$			
	LEM	HSM	M-O	Chang	LEM	HSM	M-O	Chang	LEM	HSM	M-O	Chang	LEM	HSM	M-O	Chang
20	.438	.440	.438	.426	.478	.479	.479	.656	.526	.526	.525	.511	.647	.645	.647	.629
25	.361	.362	.361	.346	.397	.398	.397	.380	.438	.438	.438	.419	.539	.539	.539	.516
30	.297	.299	.297	.279	.330	.330	.330	.310	.366	.366	.366	.344	.454	.453	.454	.426

According to stress distribution along the wall, application point of resultant force can be determined as follows:

$$\sum_{i=1}^n \{ p_i \cos(\delta + \theta) \times [\sum_{j=i}^n h_j + \frac{h_i}{2}] \} = p_a \cos(\delta + \theta) \times z_c \quad (31)$$

$$z_c = \frac{\sum_{i=1}^n \{ p_i \times [\sum_{j=i}^n h_j + \frac{h_i}{2}] \}}{p_a} \quad (37)$$

Pressure distribution along the wall being shown in Fig. 12 is determined based on proposed formulation which has the basis of Horizontal Slices Method. This method yields to nonlinear distribution. Pressure distribution for different horizontal seismic coefficients is illustrated in Fig. 13. Curves are of similar shape and as can be observed in this figure pressure increases by increase in seismic coefficient in nonlinear order. Fig. 14 demonstrates the pressure distribution determined by Horizontal

Slices Method for different angles of inclination. Nonlinear pressure distribution due to increase in slope of the wall is obvious in this figure. Also, the point of application of the pressure always shifts to the lower two-thirds of the wall height.

According to the proposed method, the pressure on the wall and angle of failure wedge have been calculated based on the difference in inclination angle of wall and seismic coefficient ( $K_h$ ) in Figs. 15 and 16.

#### 4. Comparison of the Results

Two methods have been proposed for calculating the angle of failure wedge and active pressure in inclined retaining walls. Results obtained from these two methods for determining angle of failure wedge, active pressure coefficient and depth of tensile cracks are shown in Table 3 for a wall with height of 10 meters. Investigation of results reveals the equality between angle of failure wedge estimated by both

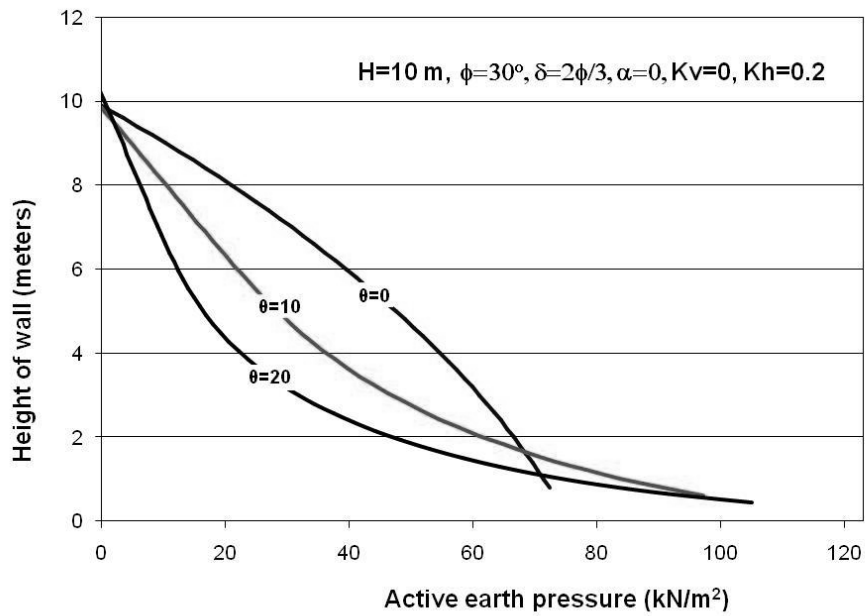


Fig. 14. Stress distribution for different inclination angles

methods. However, by increase in  $\theta$  the difference between estimated values for active pressure coefficient of a soil diverges. This difference arises from assuming the stress distribution to be linear in limit equilibrium method. Nonlinear distribution of stress will be accepted in Horizontal Slices Method.

Various relations have been proposed for calculating the active earth pressure on vertical

walls in static and pseudo-static conditions. In literature, no complete analytical solution has been observed by authors for determination of active earth pressure on inclined walls. In order to study the validity of suggested relations in present research, obtained results have been compared with findings reported by previous researchers for vertical walls retaining granular and cohesive-frictional soils.

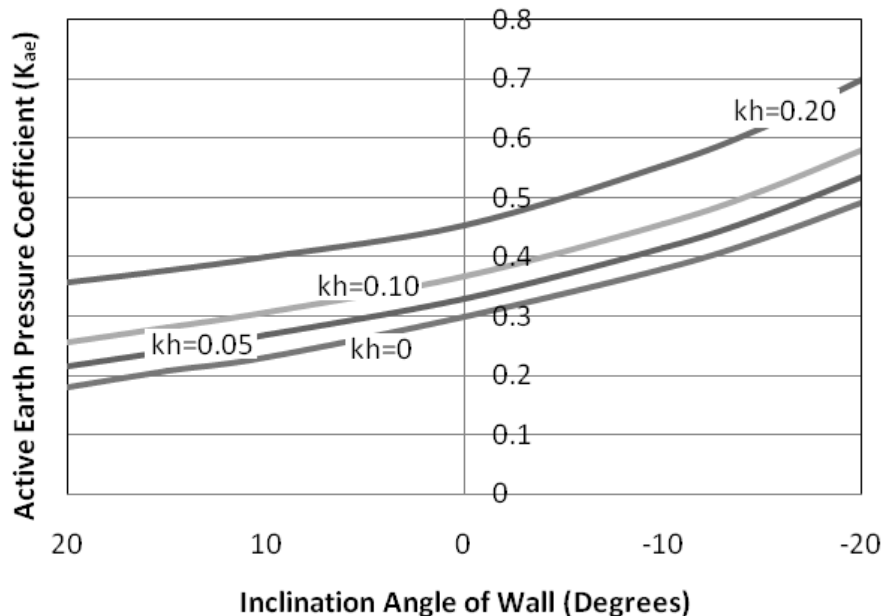


Fig. 15. Change in  $K_{ae}$  by inclination angle of wall for different  $K_h$

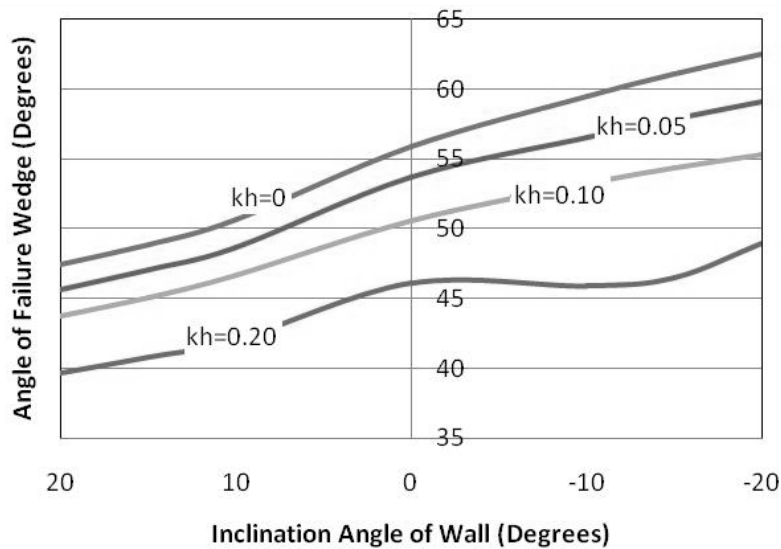


Fig. 16. Change in angle of failure wedge by inclination angle of wall for different Kh

#### 4.1. Granular Soils

Seismic pressure coefficients obtained by Mononobe-Okabe [5,6] and Cheng [13] methods is indicated in Table 4 for a vertical wall with height of 10 meters and are compared with values resulted from two proposed methods in current research. Investigation of these methods shows that for  $K_h$  being greater than 0.10 ( $K_h > 0.1$ ), all of them provide the same and agreeable results. While for seismic coefficients less than 0.10 ( $K_h < 0.1$ ) significant difference is observed between results of Cheng [13] method with others.

Estimations of various methods from the failure wedge's angle for a vertical retaining wall is indicated in Table 5. Studying these results shows pronounced harmony between predictions of different methods in all of cases. Fig. 17 illustrates estimations of failure wedge's angle by Zarabi-Kashani [7] which is been compared with results of proposed method (HSM) for a vertical

wall. As can be observed, maximum difference in mentioned methods has been about 2 degrees within the range of ordinary seismic coefficients.

#### 4.2. Cohesive-Frictional Soils

Recent studies have been contributed to solve the problem of active earth pressure on retaining walls with cohesive backfill [13, 25, 26,27]. Das and Puri [25] developed a modified method for calculating the static and seismic earth pressure behind a rigid wall by considering the cohesion between soil and wall. Gnanapragasam [26] proposed an analytical solution to determine the lateral active earth pressure distribution on a retaining wall with cohesive backfill. Unlike Rankine's method [28], his results showed that for sloping cohesive backfill the slope of the surface is a function of overburden pressure and becomes shallower with depth, thus forming a curvilinear failure surface. Cheng [13] suggested

Table 5. Comparison of results for calculation of angle of failure wedge

LEM: Proposed Method (Based on Limit equilibrium)  
HSM: Proposed Method (Horizontal slice method)  
Z-K: Zarabi-Kashani(1979)  
Chang : Chang(2003)

$$\alpha = 0^\circ, K_v = 0, c = 0, \delta = \frac{2}{3} \phi, \theta = 0$$

	$K_h=0.0$				$K_h=0.05$				$K_h=0.1$				$K_h=0.2$			
	LEM	HSM	Z-K	Chang	LEM	HSM	Z-K	Chang	LEM	HSM	Z-K	Chang	LEM	HSM	Z-K	Chang
$\phi=20$	50	49.9	50	50	47	47.1	46.6	47	43	43.9	42.8	43.0	33	36.3	33.4	33
$\phi=25$	53	52.9	53	53	50	50.5	50.1	50	47	47.8	46.9	47	39	41.7	39.4	39
$\phi=30$	55	55.9	56.0	56	53	53.7	53.4	53	51	50.6	50.5	51	44	46.1	44.1	44

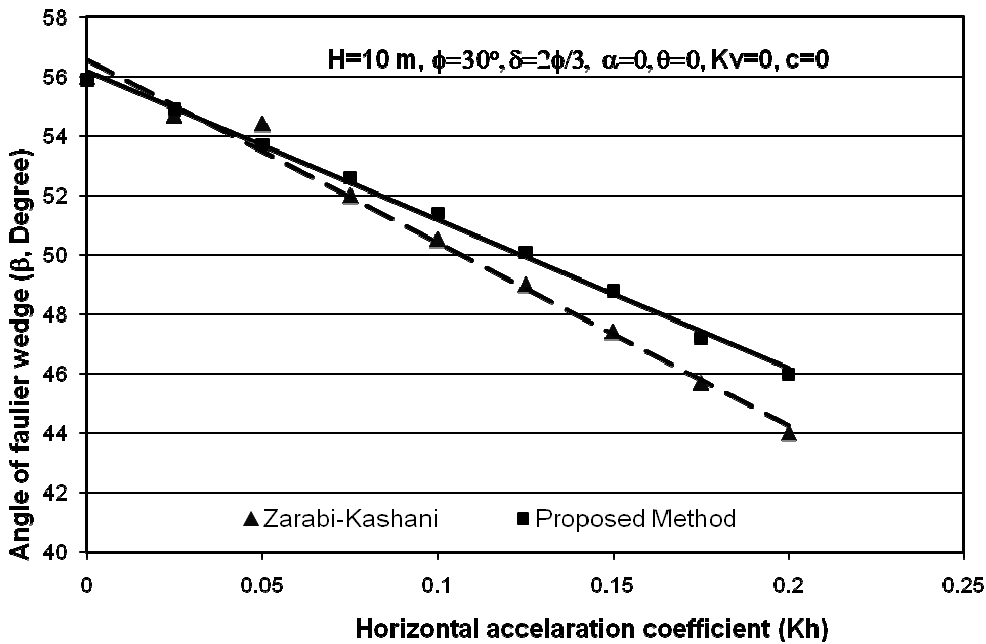


Fig. 17. Comparison of proposed method with Zarabi-Kashani (1979) method for calculating the angle of failure wedge in seismic conditions

rotation of axis for solving slip line equations to determine lateral earth pressure under general conditions. Liu et al. [27] proposed a general tangential stress coefficient to replace the Haar and Von Karman hypothesis in calculating active earth pressures. Their results showed that for any value of this coefficient, the active earth pressure converges to Rankine's solution when the radius is sufficiently large compared to the depth of wall. For cohesive frictional soils, the critical value of this coincidental coefficient is smaller than active earth pressure coefficient owing to the effect of the cohesive strength of the soil.

Table 6 compares the results of suggested

approach based on Horizontal Slices Method for cohesive-frictional soils with techniques of Das and Puri [25] and Cheng [13]. Results indicate that different methods have been in good agreement and therefore suggested formulation provides reliable predictions for vertical walls.

## 5. CONCLUSION

Active earth pressure on inclined walls is smaller in comparison with vertical ones and thus designing an inclined retaining wall will not be economical by methods originally developed for vertical walls. Lack of analytical solution for

Table 6. Comparison of results obtained from present method and solutions of Das and Puri (1996) and Chang (2003)

HSM: Proposed Method (Horizontal slice method)  
 Chang : Chang (2003)  
 D-P: Das and Puri (1996)

$\alpha = 0^\circ, K_v = 0.05K_h, \delta = \frac{2}{3}\phi, \theta = 0, \phi = 20, H = 10m, \gamma = 20KN/m^2$

C (kN/m <sup>2</sup> )	$K_h = 0.0$			$K_h = 0.05$			$K_h = 0.1$			$K_h = 0.15$			$K_h = 0.2$		
	D-P	Chang	HSM	D-P	Chang	HSM	D-P	Chang	HSM	D-P	Chang	HSM	D-P	Chang	HSM
0															
$P_a$	443	440	446	447	446	460	523	513	521	577	580	580	643	632	638
$\beta$	50	51	51	46.6	47	47	42.8	43	43.9	38.4	40.3	40.3	33.1	34	36.1
10															
$P_a$	314	313	318	337	339	345	382	380	385	433	432.9	432.9	489	479	482
$\beta$	50.6	53	52.6	48.4	49	49.35	45.6	47	46.9	42.6	44	44	39.1	40	39.7
20															
$P_a$	190	187	190	205	215	218	251	253	254	301	297.1	297.1	356	340	348
$\beta$	50.6	54	53.7	49.5	51	51.1	47.4	49	49.3	45.2	46.7	46.7	42.7	44	43.8

calculating active earth pressure on an inclined wall motivated the authors to present a new formulation based on limit equilibrium concept for a single failure wedge mechanism. This aim has been achieved by dividing the failure wedge into horizontal slices and writing equilibrium equations for all of them. In order to assess the validity of relations, comparison of results has been performed between previous methods for vertical walls and suggested approach in this paper which shows the applicability of formulation.

Findings of current research show that active earth pressure's distribution on inclined walls is of nonlinear pattern in contrast with vertical walls and hence application point of resultant force on an inclined wall is located in elevation less than one third of the height of wall being measured from its heel. On the other hand, investigation of results shows that active earth pressure ( $K_a$ ) and seismic active pressure coefficient ( $K_{ac}$ ) both increase linearly with increase in slope of retaining wall. Finally, in natural stability angle of slope, these two coefficients will be equal to zero.

In the light of what was mentioned, simplified formulation has been presented which allows calculation of active earth pressure for an inclined wall by having active earth pressure of a vertical wall coupled with its natural angle of stability. Results show the linear relation between failure wedge and slope of the wall hence simplified linear relation for its calculation has been suggested.

Presented method in this research based on limit equilibrium concept has advantages of taking into account the effect of inclination on properties of active earth pressure and also on failure wedge's angle as well as considering the effect of cohesion and friction simultaneously.

## REFERENCES

[1] Nayeri, A., Fakharian, K. (2009) "Study on Pullout Behavior of Uniaxial HDPE Geogrids under Monotonic and Cyclic Loads", *International Journal of Civil Engineering*, Vol. 7, No. 4, pp 212-223.

- [2] Abdi, M. R., Sadrnejad, S. A., Arjomand, M. A. (2009) "Clay Reinforcement Using Geogrid Embedded In Thin Layers of Sand", *International Journal of Civil Engineering*, Vol. 7, No. 4 pp 224-235.
- [3] Abdi, M. R., Parsapajouh, A., Arjomand, M. A. (2008) "Effects of Random Fiber Inclusion on Consolidation, Hydraulic Conductivity, Swelling, Shrinkage Limit and Desiccation Cracking of Clays", *International Journal of Civil Engineering*, Vol. 6, No. 4 pp 284-292.
- [4] Naeini, S. A., Ziaie\_Moayed, R. (2009) "Effect of Plasticity Index and Reinforcement on the CBR Value of Soft Clay", *International Journal of Civil Engineering*, Vol. 7, No. 2, pp 124-130.
- [5] Mononobe N, Matsuo H. (1929) "On the determination of earth pressure during earthquakes", In: *Proceeding of the World Engineering Congress*, Vol. 9, pp. 179–87.
- [6] Okabe, S. (1926) "General Theory of Earth Pressures", *J. Japan Soc. Civil Engineering*; Vol. 12, No. 1.
- [7] Zarrabi-Kashani, K. (1979) "Sliding of gravity retaining wall during earthquakes considering vertical accelerations and changing inclination of failure surface", Ms thesis, Department of Civil Engineering, Massachusetts Institute of Technology, Cambridge, MA.
- [8] Morrison Jr EE, Ebeling RM. (1995) "Limit equilibrium computation of dynamic passive earth pressure", *Canadian Geotechnical Journal*; Vol. 32, pp. 481–487.
- [9] Soubra AH. (2000) "Static and seismic passive earth pressure coefficients on rigid retaining structures", *Canadian Geotechnical Journal*; Vol. 37, pp 463–478.
- [10] Chen Y. (2000) "Practical analysis and design of mechanically-stabilized earth walls—I. Design philosophies and procedures", *Engineering Structures*; Vol. 22, pp 793–808.

- [11] Kumar J. (2001) "Seismic passive earth pressure coefficients for sands", *Canadian Geotechnical Journal*; Vol. 38, pp 876–881.
- [12] Kumar J, Chitikela S. (2002) "Seismic passive earth pressure coefficients using the method of characteristics", *Canadian Geotechnical Journal*; Vol. 39, pp 463–471.
- [13] Cheng Y.M. (2003) "Seismic lateral earth pressure coefficients for C- $\phi$  soils by slip line method", *Computers and Geotechnics*; Vol. 30, pp 661-670.
- [14] Yang, X.-L. and Yin, J.-H. (2006) "Estimation of seismic passive earth pressures with nonlinear failure criterion", *Engineering Structures*; Vol. 28, pp 342–348.
- [15] Choudhury D, Nimbalkar S.S. (2006) "Pseudo-dynamic approach of seismic active earth pressure behind retaining wall", *Geotechnical and Geological Engineering*, Springer, The Netherlands; Vol. 24, No. 5, pp 1103-1113.
- [16] Mylonakis G, Kloukinas P, Papatonopoulos C. (2007) "An Alternative to the Mononobe-Okabe Equation for Seismic Earth Pressures", *Soil Dynamics and Earthquake Engineering*; Vol. 27, No. 10, pp 957-969.
- [17] Yepes V, Alcalá J, Perea C, Gonzalez-Vidoso F. (2008) "A parametric study of optimum earth-retaining walls by simulated annealing", *Engineering Structures*; Vol. 30, pp 821–830.
- [18] Shahgholi M, Fagher A, Jones C.J.F.P. (2001) "Horizontal slice method of analysis", *Geotechnique*; Vol. 51, No. 10, pp 881-885.
- [19] Nouri H, Fagher A, Jones C.J.F.P. (2006) "Development of horizontal slice method for seismic stability analysis of reinforced slopes and walls", *Geotextiles and Geomembranes*; Vol. 24, pp 175–187.
- [20] Shekarian S, Ghanbari A, Farhadi, A. (2008) "New seismic parameters in the analysis of retaining walls with einforced backfill", *Geotextiles and Geomembranes*; Vol. 26, No. 4, pp 350–356.
- [21] Nouri H, Fagher A, Jones C.J.F.P. (2008) "Evaluating the effects of the magnitude and amplification of pseudo-static acceleration on reinforced soil slopes and walls using the limit equilibrium horizontal slices method", *Geotextiles and Geomembranes*; Vol. 26, No. 3, pp 263–278.
- [22] Azad A, Yasrobi S, Pak A. (2008) "Seismic active earth pressure distribution behind rigid retaining walls", *Soil Dynamic and Earthquake Engineering*; Vol. 28, No.5, pp 365-375.
- [23] Shekarian S, Ghanbari A. (2008) "A Pseudo-Dynamic Method to Analyze Retaining Wall with Reinforced and Unreinforced Backfill ", *JSEE*; Vol. 10, No. 1, pp 41-47.
- [24] Segrestin P. (1992) "Design of sloped reinforced fill structure", In: *Proceedings of Conference on Retaining Structures*, Institute of Civil Engineering, Robinson College, Cambridge, pp 574–584.
- [25] Das B.M, Puri V.K. (1996) "Static and dynamic active earth pressure. *Geotechnical and Geological Engineering*"; Vol. 14, pp 353-366.
- [26] Gnanapragasam G. (2000) "Active earth pressure in cohesive soils with an inclined ground surface", *Canadian Geotechnical Journal*; Vol. 37, pp 171-177.
- [27] Liu, F.Q., and Wang, J.H. (2008) "A generalized slip line solution to the active earth pressure on circular retaining walls", *Computers and Geotechnics*; Vol. 35, No. 2, pp 155–164.
- [28] Rankine W. J. M. (1857) "On the mathematical theory of the stability of earthwork and Masonry", *Proceedings of Royal Society*, Vol. 8.